

Tensile properties of mechanically alloyed Zr added austenitic stainless steel

Daniel Morrall^{a,*}, Jin Gao^b, Zhexian Zhang^b, Kiyohiro Yabuuchi^b, Akihiko Kimura^b, Takahiro Ishizaki^c, Yusaku Maruno^c

^a Graduate School of Energy Science, Kyoto University, Yoshida-honmachi, Sakyou-ku, Kyoto 606-8501, Japan

^b Institute of Advanced Energy, Kyoto University, Gokasho, Uji, Kyoto 611-0011, Japan

^c Hitachi, Ltd. Research & Development Group, Hitachi, Ibaraki 319-1292, Japan

ARTICLE INFO

Keywords:

Powder metallurgy
Grain size effect
Precipitation hardening
Zr-oxides

ABSTRACT

A mechanically alloyed austenitic stainless steel (MA304LZ) was produced from pre-alloyed SUS304L powder with a small amount of Zr addition. The yield stress of MA304LZ was more than 3 times larger than that of SUS304L or 316L, while total elongation was reduced to about one third of the conventional steels. Microstructure analysis revealed an average grain size of 0.42 μm in MA304LZ and about 34/30 μm in SUS304L/316 L. In MA304LZ, two types of precipitates were observed; inhomogeneously distributed fine precipitates with an average size of 6.0 nm and homogeneously distributed coarse precipitates ($d > 20$ nm) with an average size of 47 nm. The strengthening mechanism of MA304LZ was discussed on the bases of Hall-Petch and Orowan equations, and the strengthening of MA304LZ was attributed mostly to refined grains. The dislocation barrier strength factor, α , is estimated to be 0.277 for the Zr-rich precipitates in MA304LZ.

1. Introduction

Oxide dispersion strengthened (ODS) austenitic stainless steels have been considered as a new candidate material for high burn-up fuel cladding of next generation nuclear power plants [1]. During a high burn-up operation, zircaloy is corroded in an anodic reaction with accompanying hydrogen generation as a cathodic reaction which may cause hydrogen embrittlement and consequently reduces the lifetime of the cladding. Since austenitic stainless steels are generally corrosion resistant due to the high Cr and Ni content, the steels were considered to be more adequate than zircaloy for high burn-up fuel claddings [2,3]. However, the yield stress (YS) of austenitic stainless steels is much smaller than zircaloy, which requires improvement. Furthermore, the steels suffer from severe void swelling with a much higher swelling rate than ferritic steels [4,5]. The severe swelling of austenitic steels can be improved by the dispersion of nano-particles and the addition of oversized elements, which may greatly suppress the clustering of vacancies by trapping vacancies and small vacancy clusters at the interfaces of particle and matrix of the steel [6,7].

Various previous studies on dispersion strengthened austenitic stainless steels have shown improvement in several areas. Wang et al. fabricated ODS-304 steel by mechanical alloying and obtained a higher YS of 525 MPa for as HIPed condition and 595 MPa for HIP plus forging condition [1]. Miao et al. conducted a microstructural observation study for mechanically alloyed ODS-316 steel, and they achieved a high

YS of 477 MPa at RT and 328 MPa at 550 °C in the as HIPed condition [8]. More recently, Gräning et al. investigated mechanical properties of two different mechanically alloyed austenitic stainless steels with different chemical compositions, amounts of Zr addition, and alloying conditions: and found that both steels opposed a rather high ultimate tensile strength although the YS appeared to be not so high from the results of hardness measurement [9]. Although the strengthening is considered to be due to the refinement of grain size and precipitation of small oxide particles, the contribution of each strengthening factor is not clear.

In ODS ferritic steel, a small amount of Zr addition reduced the size and increased the number density of oxide particles, and consequently increased the YS of the ODS ferritic steels significantly [10]. Accordingly, it is expected that the mechanically alloyed austenitic stainless steel with an addition of a small amount of Zr bears high strength with good resistance to SCC as well as void swelling.

In this work, we fabricated a mechanically alloyed austenitic stainless steel with high strength, and the strengthening mechanism was discussed to clarify the contribution of strengthening factors, that is, grain refining and precipitation hardening in the mechanically alloyed austenitic stainless steel with a small amount of Zr addition.

2. Experimental

The materials used were a mechanically alloyed austenitic stainless

* Corresponding author.

E-mail address: moraru.danieru.43v@st.kyoto-u.ac.jp (D. Morrall).

<https://doi.org/10.1016/j.nme.2018.03.002>

Received 15 December 2017; Received in revised form 7 February 2018; Accepted 7 March 2018

2352-1791/ © 2018 Elsevier Ltd. This is an open access article under the CC BY-NC-ND license (<http://creativecommons.org/licenses/by-nc-nd/4.0/>).

Table 1
Chemical compositions of MA304LZ, SUS304L and SUS316L.

	C	Si	Mn	P	S	Cr	Ni	Zr	O	N	Fe
MA304LZ	0.02	0.98	0.15	0.018	0.001	19.5	11.18	0.7	0.018	0.074	Bal
SUS304L	.03	.59	0.99	0.031	0.002	18.4	9.71	–	0.004	0.051	Bal
SUS316L	.01	0.73	1.06	0.032	0.004	17.4	12.13	–	0.002	0.032	Bal

steel with a small amount of Zr addition (MA304LZ) and two conventional austenitic stainless steels, SUS304L and SUS316L. The MA304LZ was produced from pre-alloyed SUS304L powder and high purity Zr powder of 0.7 wt. %. The mixed powder was obtained by milling in a P-5 Fritsch planetary ball mill at 200 rpm for 48 hours in an argon environment with a ball-to-powder ratio of 9:10 in weight. Both the milling balls and milling chamber were composed of SUS304 stainless steel. A rather low ball-to-powder ratio along with low rotation speed was used to alleviate the affixing issue of the resulting powder to the mixing pot [1]. The milled powder was then consolidated through hot isostatic pressing (HIP) at 140 MPa and 950 °C followed by annealing at 1000 °C for 30 min and finally quenched into water. The chemical compositions of all materials are listed in Table 1. X-ray diffraction spectroscopy (XRD) was carried out on the consolidated MA304LZ to identify the phase of the steel. XRD measurements were taken using a Rigaku RINT-TTRIII/KE XRD in the range of $2\theta = 5^\circ - 120^\circ$ with use of Co-K α at 250 mA and 40 kV.

Plate type dog-bone shape tensile specimens of which the gage portion measures 5 mm length, 1.2 mm width and 0.5 mm thickness were fabricated by an electric discharge machining. Tensile tests were carried out at a displacement rate of 0.2 mm/min at temperatures from RT to 500 °C in a vacuum of 2.7×10^{-2} Pa. The fractured surface of the tensile tested specimen was observed by SEM to determine fracture mode and reduction in area (RIA).

Transmission electron microscopy (TEM) utilizing JEM 2010 and 2200FS was used for characterizing grain size and precipitation morphology such as the number density and averaged particle size. Foil specimens were prepared with a Struers twinjet electropolisher at 18 V in a 90% CH₃OH 10% HClO₄ electrolyte at –20 °C. Grain size was evaluated by means of line intercept method with a grid of 21 lines. The number density of precipitates was estimated in a grain with thickness estimated by convergent beam electron diffraction (CBED) method.

3. Results

3.1. Tensile Properties

Stress-strain behavior of MA304LZ, SUS304L and SUS316L at RT and 500 °C is shown in Fig. 1, which indicates that, at RT, the YS of MA304LZ is significantly larger than that of SUS304L and SUS316L, although the total elongation of MA304LZ is smaller than those of conventional steels. Work hardening is significant in SUS304L, which is considered to be due to deformation-induced martensitic transformation, and resultantly the ultimate tensile stress (UTS) is similar between MA304LZ and SUS304L. At 500 °C, similar trends with those at RT were observed, while a reduction of strength was observed in all materials reflecting test temperature dependence of the materials, which is shown in Fig. 2. Room temperature YS of MA304LZ was greater by a factor of 3.8 and 3.3 for 316L and 304L, respectively. This difference in YS, $\Delta\sigma$, between MA304LZ and SUS304L is 531 MPa. At 500 °C, YS of MA304LZ was greater by a factor of 4.5 and 4.4 for 316L and 304L, respectively. The total elongation of MA304LZ reduces with test temperature from 30% to 10% accompanied by a reduction in uniform elongation.

The fractured surface of each steel at RT is shown in Fig. 3,

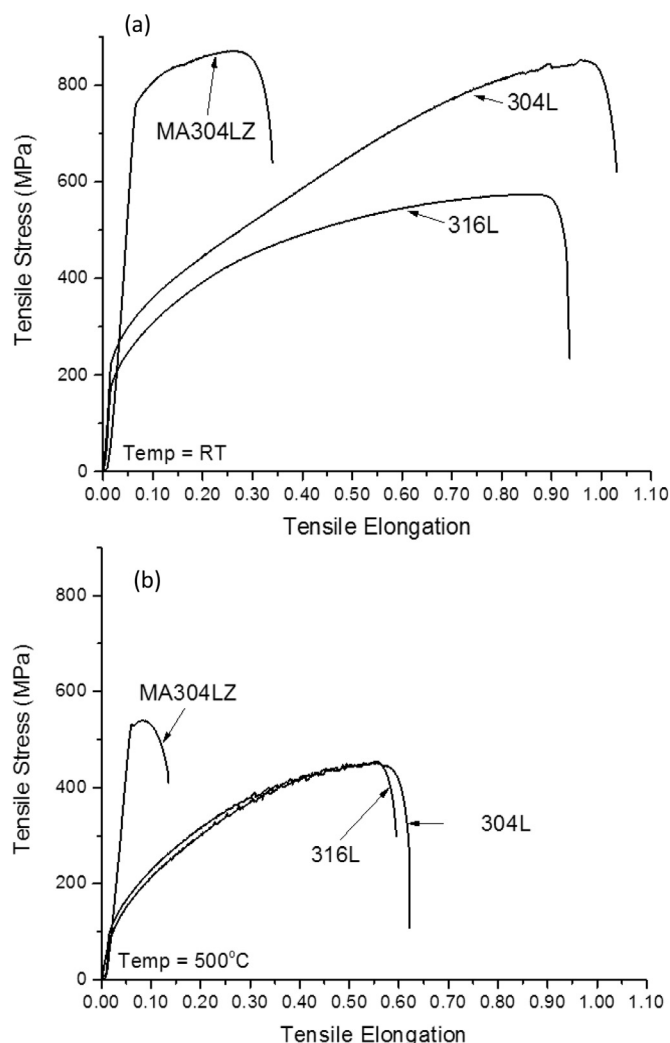


Fig. 1. Stress-strain behavior of MA304LZ, SUS304L and SUS316L deformed at (a) RT and (b) 500 °C.

indicating that all steels show ductile fracture mode. The reduction in area (RIA) of MA304LZ, 304L and 316L at RT is about 70%, 77% and 85%, respectively. The tensile properties of MA304LZ, SUS304L and SUS316L are summarized in Table 2.

3.2. Microstructure observation

Although the mixed powder was of pre-alloyed SUS304L, the phase structure was identified for the consolidated material by XRD. The XRD spectrum of MA304LZ is shown in Fig. 4, indicating that the spectrum is of FCC with an average lattice parameter measured to be 0.358 nm, which is almost the same as SUS304L [11]. The peak at 52.20 (2θ) is possibly related to the (110)_c phase.

Download English Version:

<https://daneshyari.com/en/article/7987297>

Download Persian Version:

<https://daneshyari.com/article/7987297>

[Daneshyari.com](https://daneshyari.com)